

Quantum Information Processing

Fourier Transforms and Grover's Algorithm

Evan Berkowitz

evan_b@mit.edu

Junior, MIT Department of Physics

May 15, 2007

We measure the natural NMR timescales T_1 and T_2 of the hydrogen and carbon in chloroform using a 200.13MHz NMR system. Additionally, we discuss the Grover algorithm for database search in $\mathcal{O}(\sqrt{n})$ time, and successfully implement a search of a four-entry database using those nuclei as qubits.

1. COMPUTATIONAL COMPLEXITY

A quantum computer offers a considerable speed up for solving some problems by operating on all the possible inputs at once via superposition instead of looping over them one at a time as a classical computer must. But what is meant by “speed up”? Surely the amount of watch time an algorithm takes is not a good measure of its speed—the same algorithm on classical computers with different processors could take different amounts of time. Instead, we count the number of steps an algorithm takes to execute and define this to be the “time”. An algorithm’s running time is usually expressed in terms of the size of the input, n , to show how the time grows as a function of the input.

Computer scientists specify complexity using Big-O notation, which gives an asymptotic upper bound on the running time up to a multiplicative constant. For instance, we say that the function $f(x) = 2x^2 + 3x + 10$ is $\mathcal{O}(x^2)$ because for an appropriate multiplicative constant c and large enough x , cx^2 is greater than or equal to $f(x)$. Similarly, that particular $f(x)$ is also $\mathcal{O}(x^3)$, because for large enough x , x^3 is always greater than $f(x)$. [1]

If we consider the problem of searching through a database of size n for a unique entry (called the *winner*), it is natural to expect that the best we can do classically is $\mathcal{O}(n)$, since we may have to check each entry before finding the winner. Even on average, we expect to query the database $\frac{n}{2}$ times, and we ignore the multiplicative factor of $\frac{1}{2}$ in Big-O notation.

Interestingly, a quantum computer can search a database in only $\mathcal{O}(\sqrt{n})$ via Grover’s algorithm. We note, particularly, that $\sqrt{n} = \mathcal{O}(n)$ but $n \neq \mathcal{O}(\sqrt{n})$, revealing that the quantum algorithm is inherently faster than the classical algorithm.

2. EXPERIMENTAL APPARATUS

We implemented the quantum computation on a Bruker Avance 200 NMR device. This NMR machine had a strong 200.13 MHz static magnetic field, which describes the Larmor frequency of hydrogen in the field. Equivalently, we can describe the magnetic field as be-

ing 4.7 Tesla. This field strength is consistent over the sample to better than 1 part in 10^9 . [2]

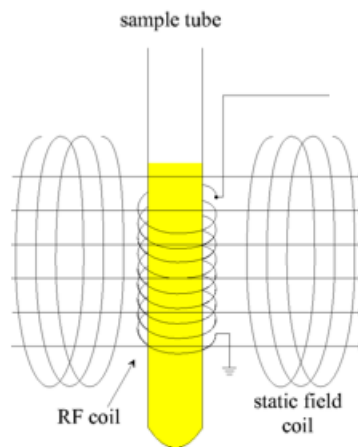


FIG. 1: A schematic NMR setup. [2]

We placed a sample of $^{13}\text{CHCl}_3$ dissolved in d6-acetone into the NMR device in a flame-sealed tube. The tube was mounted on a circular spinner, which allowed the sample to be spun, averaging away inhomogeneities in the magnetic field. The deuterium provided the setup with a signal which could be used to ensure the strength of the magnetic field was consistent in time via an active feedback loop. The $^{13}\text{CHCl}_3$ provided the two qubits: coupled hydrogen and carbon nuclei via spin-spin interaction.

The setup was then connected to a signal chain which communicated with Bruker xwin-nmr control software, which was further abstracted into a Matlab interface via a home-grown software package. A schematic of the setup can be seen in Fig. 2.

3. FOURIER TRANSFORMS

As in any NMR device, we read information about the nuclear spins by measuring free induction decays or FIDs. The Matlab package used automatically converted the signal received in time into a frequency spectrum via a discrete Fourier transform. Thus, it is important to

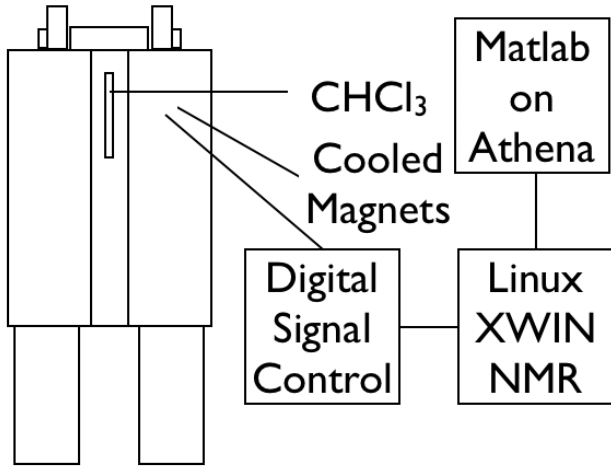


FIG. 2: A block diagram of our experiment.

understand the correspondence between an FID and a frequency spectrum. A typical FID-frequency spectrum pair is shown in Fig. 3.

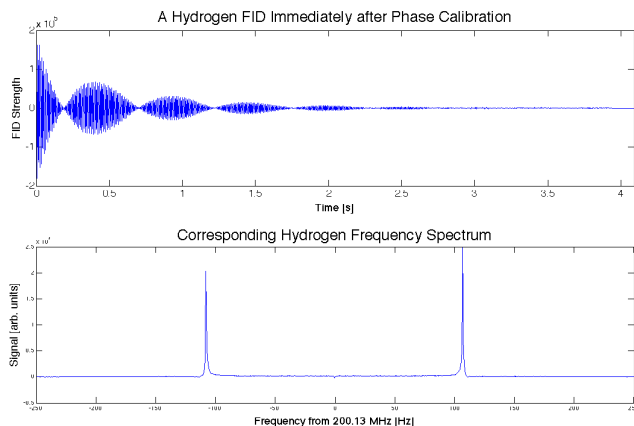


FIG. 3: A typical hydrogen FID

By examining the FID we observe a few phenomena. First, we see obvious exponential decay, as is expected of a free induction decay. Second, we see obvious beating of the sinusoidal signal, with frequencies ω_0 and $\Delta\omega$, describing the fast and slow oscillations respectively.

It can be shown that this beating can be decomposed into two frequencies via the identity

$$\sin \omega_1 t + \sin \omega_2 t = 2 \cos \frac{\omega_1 - \omega_2}{2} t \sin \frac{\omega_1 + \omega_2}{2} t, \quad (1)$$

or equivalently

$$\sin(\omega_0 + \Delta\omega)t + \sin(\omega_0 - \Delta\omega)t = 2 \cos \Delta\omega t \sin \omega_0 t. \quad (2)$$

which describes the spectrum in Fig. 3 well.

Since the Fourier transform of $f(t)$,

$$F(\omega) = \frac{1}{\sqrt{2\pi}} \int_{-\infty}^{\infty} dt e^{-i\omega t} f(t) \quad (3)$$

is linear in $f(t)$, we should expect the frequency spectrum of (2) to be a simple sum of the transforms of each term. Using Fourier transform tables, we find that we should get two Lorentzians (accounting for the exponential decay) centered at $\omega_0 \pm \Delta\omega$. This is confirmed by the spectrum in Fig. 3.

The two frequencies may be interpreted semi-classically. The primary 4.7 Tesla field causes a frequency ω_0 . Then, one nucleus' magnetic moment adds a field either parallel or antiparallel to the primary field at the site of the second nucleus. This change in the field, small compared to 4.7 Tesla, causes a change in the frequency of the second nucleus—if the added field is parallel to the primary field, the frequency grows by $\Delta\omega$, and if the added field is antiparallel the frequency decreases by the same amount. If we see only one peak (for instance, in Fig. 5) we can understand this to mean that only one configuration of the moments is present.

4. NATURAL TIMESCALES AND RELIABLE COMPUTATION

For reliable computation, we demand the natural NMR timescales which describe the decoherence of the ensemble be much longer than the computing time.

By examining the spectra taken immediately after phase calibration, we can determine the full width at half max of the Lorentzians Γ . We use these spectra because they have the smallest imaginary parts, and any imaginary part can change the appearance of those peaks. A typical spectrum of this type is shown in Fig. 3. For hydrogen peaks we find $\Gamma = 0.7 \pm 0.1$ Hz and for carbon we find $\Gamma = 1.4 \pm 0.1$ Hz. These Γ correspond to T_2 of 1.4 ± 0.2 s and 0.7 ± 0.1 s for hydrogen and carbon respectively. T_2^* will approximately equal to T_2 , because as mentioned earlier the field is constant to better than 1 part in 10^9 and the sample is spun to further reduce the effects of inhomogeneities of the field.

The timescale T_1 was found via inversion recovery, or a $180-\tau-90$ pulse sequence. The inverted ensemble recovers after a time τ and then is subjected to an additional $\frac{\pi}{2}$ pulse. If the ensemble has recovered exactly 50%, the net spin will be exactly against the primary field, yielding no FID. Since T_1 is the time it takes to recover by a factor of e , we multiply this time by a factor of $\ln 2$. For hydrogen, the data is shown in 4. We determined T_1 to be 12.37 ± 0.04 s and 11.84 ± 0.07 s for the right and left hydrogen peaks, respectively. The two peaks have different T_1 due to the different environments they experience, as suggested by the semi-classical model described earlier. For carbon, similar calculations give T_1 to be 15.6 ± 0.6 s and 12.9 ± 0.6 s for the right and left peaks, respectively.

We have shown that all relevant decoherence timescales are on the order of at least seconds. Now we must show that this time is much greater than the time required to do a computation. Our algorithm can be broken down into $\frac{\pi}{2}$ pulses, and will be discussed in Sec. 6. Since our

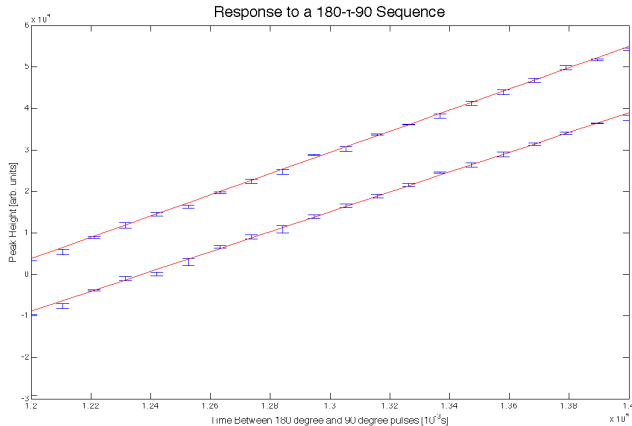


FIG. 4: Linear fits of the hydrogen peak size.

computations only require a small number of pulses, if the time for the $\frac{\pi}{2}$ pulses is much shorter than 1 second (the order of the natural timescales) we will be able to run our algorithm successfully. We previously determined the $\frac{\pi}{2}$ pulse widths to be $9.3 \pm 0.2 \mu\text{s}$ and $8.8 \pm 0.3 \mu\text{s}$. [3] Using similar techniques we were unable to significantly improve our numbers, even with detailed probing of the small around these values. When probing the times close to the previously measured values we obtained a large amount of noise, even five measurements at each time. We sampled thirty times from 9.1 to $9.5 \mu\text{s}$, obtaining essentially a flat line. With these additional data, we are only able to decrease the error for the $\frac{\pi}{2}$ pulse width of hydrogen a small amount—we measure it to be $9.35 \pm 0.15 \mu\text{s}$. We were unable to find a better value than $8.8 \pm 0.3 \mu\text{s}$ with a similar measurement. As these pulse widths are much shorter than 1s, we can compute without concern for the effects of decoherence.

5. COMPUTATIONAL BASIS STATES

Using a technique known as thermal averaging it is possible to take multiple spectra and extract from them how the ensemble would behave if the spins were not distributed according to the statistical-mechanical partition function but instead were all in a single state.[2] Thus, by applying the thermal averaging method, we can extract the true behavior of the two qubits without struggling with the interpretation of the thermal distribution.

We can observe either nucleus—either will provide a full picture of the state of the system. In this experiment we chose to observe the carbon nucleus. The four computational basis states are shown in Fig. 5.

We label the four basis states with two labels, one for each nucleus. If a nucleus is up, then we label it with a 0, and if it is down, with a 1. Thus, the four states are given by $|00\rangle$, $|01\rangle$, $|10\rangle$, and $|11\rangle$. We relabel these states by treating their label as a binary value and con-

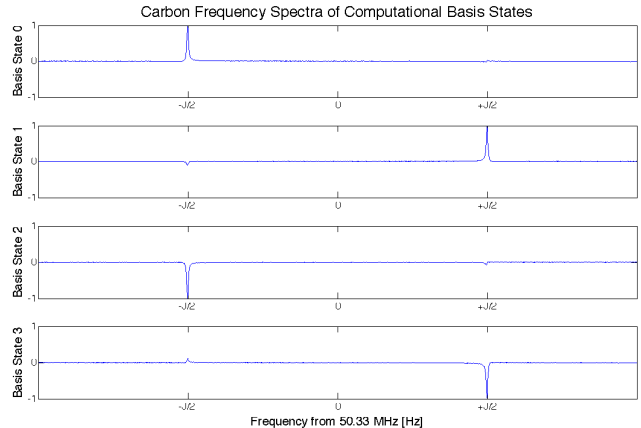


FIG. 5: The four basis states of carbon. Note that the y-axis is rescaled, as the signal strength is arbitrary anyway.

verting it to decimal. Thus, the states are equivalently called $|0\rangle$, $|1\rangle$, $|2\rangle$, and $|3\rangle$ respectively.

6. GROVER'S ALGORITHM

Suppose we had a database of size n , with one unique entry, the winner. If the database entries are labeled 0 to $n - 1$, then we specify the winner's uniqueness with a function $f(x)$ which gives 0 on all x except for the winner, in which case f gives 1. In Sec. 1 we discussed that classical database search is $\mathcal{O}(n)$. In this case, we mean that we must evaluate f on the order of n times before finding the winner. Finding the winner is the same as determining f . We do not know the inner workings of f , because otherwise we would not need to search the database at all.

We implement f quantum-mechanically with an operator called an oracle. The oracle is a diagonal operator which treats all of the entries (states) equally, except for the winner $|w\rangle$. The oracle which would make $|3\rangle$ unique is

$$O_3 = \begin{pmatrix} 1 & 0 & 0 & 0 \\ 0 & 1 & 0 & 0 \\ 0 & 0 & 1 & 0 \\ 0 & 0 & 0 & -1 \end{pmatrix}. \quad (4)$$

The implementation of the four different oracles are shown as NMR pulse sequences in Table I. The operator R refers to a rotation of $\frac{\pi}{2}$, the numerical subscripts describe which qubit is being rotated, and the letter subscript describes the axis about which the qubit is rotated, with an overbar representing a rotation about the opposite axis. For instance, R_{x1} is a $\frac{\pi}{2}$ rotation of the first qubit about the x -axis and $R_{\bar{y}2}$ is $\frac{\pi}{2}$ a rotation of the second qubit about the $-y$ -axis. The operator τ denotes waiting a time equal to the free evolution period, $\frac{1}{2J}$. J

was previously determined to be 215.18 ± 0.12 Hz, with the error limited by the width of a bin.[3]

TABLE I: The pulse sequences giving rise to the four oracles.

Oracle	Operator Sequence
O_0	$R_{\bar{y}2}R_{x2}R_{y2}R_{\bar{y}1}R_{x1}R_{y1}\tau$
O_1	$R_{\bar{y}2}R_{\bar{x}2}R_{y2}R_{\bar{y}1}R_{\bar{x}1}R_{\bar{y}1}\tau$
O_2	$R_{\bar{y}1}R_{x1}R_{y1}R_{y2}R_{\bar{x}2}R_{\bar{y}2}\tau$
O_3	$R_{y1}R_{x1}R_{\bar{y}1}R_{y2}R_{x2}R_{\bar{y}2}\tau$

Additionally, we use the Hadamard gate H^{\otimes} given by

$$H^{\otimes} = \frac{1}{\sqrt{2}} \begin{pmatrix} 1 & 1 \\ 1 & -1 \end{pmatrix} \otimes \frac{1}{\sqrt{2}} \begin{pmatrix} 1 & 1 \\ 1 & -1 \end{pmatrix} \quad (5)$$

which takes the state $|0\rangle$ and maps it into an equal super position of all computational basis states $|s\rangle$:

$$|s\rangle = H^{\otimes} |0\rangle = \frac{1}{\sqrt{n}} \sum_{a=0}^{n-1} |a\rangle, \quad (6)$$

which generalizes to systems with more than 2 qubits. The state $|s\rangle$ is in some sense the database we wish to search: it contains an equal amount of each database entry.

Finally, we need the operator P

$$P = -O_0 \quad (7)$$

which is the conditional phase-shift operator, which allows us to interfere the different paths of computation.

A Grover iteration G is given by $H^{\otimes}PH^{\otimes}O_w$, where O_w is oracle whose subscript we wish to determine. To determine the complexity, we count the number of Grover iterations (and thus the queries of the oracle), k . If we let $|\psi_k\rangle$ be the state $G^k|s\rangle$, then we find

$$\langle w | \psi_k \rangle \approx \sin((2k+1)\theta) \quad (8)$$

with

$$\sin \theta = \frac{1}{\sqrt{n}}. \quad (9)$$

Thus, we find that in a 2-qubit system ($n=4$), $\theta = \frac{\pi}{6}$ and thus with only one application of G we have a very large probability of finding the winner.[2]

From Eq. (8) it is clear that we wish $(2k+1)\theta$ to be approximately $\frac{\pi}{2}$. For large n , we note that $\theta \approx \frac{1}{\sqrt{n}}$ and thus to get a high probability of success we should apply G k times, given by

$$k \approx \frac{\pi}{4} \sqrt{n}. \quad (10)$$

Since we consider k to be the measure of complexity, in that it counts how many times we apply the oracle, we see that Grover's algorithm is $\mathcal{O}(\sqrt{n})$, faster than any classical algorithm.

7. RESULTS

We applied the four Grover operations to the state $|s\rangle$ once. As predicted, applying the 0^{th} oracle led us to measure primarily $|0\rangle$, the 1^{st} oracle led us to measure primarily $|1\rangle$, etc. with high probability. Compare Fig. 5 and Fig. 6 to see the strong likeness between the computational basis states and the states found by the Grover operations. This confirms the success of our quantum algorithm.

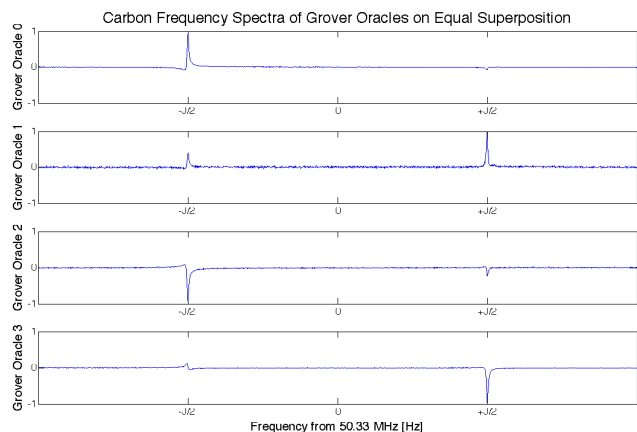


FIG. 6: The four states which result from having the different Grover oracles applied to the database.

8. CONCLUSIONS

We have shown that all relevant physical timescales which might interrupt our computations are much longer than the timescale required to do those computations successfully. Additionally, we have discussed the Grover algorithm for searching a database of size n in $\mathcal{O}(\sqrt{n})$ time and have successfully implemented it on a four-entry database via a two-qubit pulsed NMR system. This speed up is fundamentally quantum-mechanical, and demonstrates the advantage quantum computation holds over classical computation.

[1] M. Sipser, *Introduction to the Theory of Computation* (Thomson Course Technology, 2006), chap. 7, p. 249, 2nd

- [2] S. Sewell, *Quantum Information Processing with NMR*, <http://web.mit.edu/8.13/www/JLExperiments/JLExp49.pdf> (2007).
- [3] E. Berkowitz, *Quantum Information Processing*, http://web.mit.edu/~evan_b/Public/8.13/Papers/QIP.pdf (2007).